

Robust high-dimensional morphological metric: application to the ADNI multi-centric dataset

N. Robitaille¹, A. Mouihha¹, and S. Duchesne^{1,2}

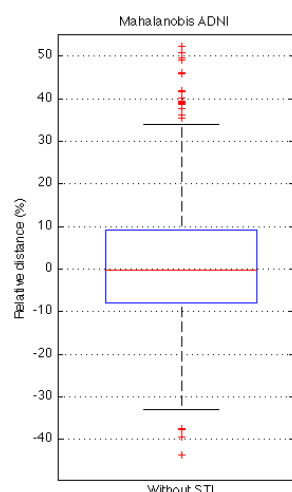
¹Centre de recherche Université Laval Robert-Giffard, Québec, QC, Canada, ²Radiology, Université Laval, Quebec, QC, Canada

INTRODUCTION

Early detection of Alzheimer's dementia (AD), critical for treatment success, is a high priority research area. The development of disease-modifying treatment strategies requires objective characterization techniques and quantitative biomarkers able to identify AD with higher accuracy and at a much earlier stage than clinically based assessment [1]. Given that structural magnetic resonance imaging (MRI) (e.g. T1 -weighted) on 1 to 3 Tesla clinical scanners allows the *in vivo* assessment of these changes, it has been proposed to fulfill the role of quantitative biomarker in AD [2-4]. To this end we have proposed a single, high-dimensional morphological metric called the *disease evaluation factor* (DEF) extracted from T1-weighted MRI and estimated its efficiency in discriminating cognitively normal, control subjects (CTRL) from probable AD patients in a single-center setting [5]. However, multi-centric research studies (e.g. the Alzheimer's Disease Neuroimaging Initiative or ADNI [6]) and especially clinical applications (e.g. trials and care) require any metric to be robust to scanner-dependent signal variations, which blur the intensity correspondence between tissue classes across images. In this report we demonstrate the robustness of our DEF metric through analysis of within-session scan-repeat scan images from the multi-centric ADNI setting and estimate the cohort size increase at various difference levels due to this minimum detection threshold.

METHOD

Datasets – In this study we used data from three different studies, totaling 1097 subjects from 58 centers, with respective IRB approvals. First, we required two independent subject groups to build our high-dimensional metric. The first was the *Mapping group*, consisting in 150 subjects from the ICBM database [7], and scanned in Montreal, Canada on a Philips Gyroscan 1.5T scanner (Best, Netherlands) using a T1-weighted fast gradient echo sequence (sagittal acquisition, TR=18 ms, TE=10 ms, 1mm X 1mm X 1mm voxels, flip angle 30°). The second was the *Classification group*, which consisted in 75 probable AD and 75 CTRL subjects from the LENITEM database [8], scanned in Brescia, Italy on a single Philips Gyroscan 1.0T scanner (Best, Netherlands) using a T1-weighted fast field echo sequence (sagittal acquisition, TR=25 ms, TE=6.9 ms, 1mm X 1mm X 1.3mm voxels). Finally, the *Test group* consisted in 1594 baseline MRIs (scan + same-session repeat scans) from 797 CTRL, mild cognitive impairment and probable AD subjects participating in ADNI, acquired on 56 different 1.5T scanners using a similar 3D T1-weighted MP-RAGE protocol [9].



Initial image processing - We processed all MRI volumes identically using the MINC image processing toolbox (<http://www2.bic.mni.mcgill.ca>) and local software as follows: a) noise removal [10]; b) raw scanner intensity inhomogeneity correction [11]; c) global registration (12 degrees of freedom) [12] to the reference image space defined by the BrainWeb T1-weighted image [13] (1-mm resolution, 0% noise, 0% non-uniformity), maximizing the mutual information between the two volumes [14]; d) resampling to a 1-mm³ isotropic grid; e) linear clamping to a set [0-100] intensity range; f) non-linear registration of individual standardized subject images to the BrainWeb reference; and g) computation of determinants of the Jacobian of the deformation field [15].

Mapping and classification spaces - We generated a low-dimensional feature space with the *Mapping group* using Principal Components Analysis (PCA) of (a) T1w MRI intensity z-score maps, as a proxy of tissue composition; and (2) log-determinants maps, as a proxy of tissue atrophy. We then projected identical data from the *Classification group* into the space defined by the PCA vectors, and used a system of supervised linear classifiers to identify a restricted set of eigenvectors $\{\lambda_r\}$ forming an hyperplane that best separated the two classes under study (CTRL vs. probable AD). Finally, we projected ADNI scan/repeat scan data in the $\{\lambda_r\}$ eigenvector space.

High-dimensional metric - The morphological DEF metric is based on the concept of distance within the space defined by eigenvectors $\{\lambda_r\}$. Specifically, we calculated the Mahalanobis distance for each ADNI subject scan/repeat scans to the origin of the high-dimensional space, and then the difference between each each scan/repeat scan pairs. Finally, we estimated the minimum trial size required to detect an effect superior to that threshold using conservative power assumptions.

RESULTS

Over the 797 subjects of the ADNI dataset, the average scan/repeat scan distance was 1.7% (95% CI: 0.1% – 3.3%) (see figure). As reported previously [5], the difference in DEF averages between probable AD and CTRL was 15%. At this level, the minimum trial size required to detect this difference is 59 individuals for both samples ($\alpha = 0.05$; $\beta = 0.50$). Due to the 1.7% minimum precision threshold of the technique, to reach identical power the trial size must increase to 75 individuals.

CONCLUSION

We proposed a high-dimensional morphological metric and demonstrated its robustness in a multi-centric setting. While the resulting minimum precision threshold resulted in increased number of subjects, trial sizes remain vastly inferior to other metrics, e.g. neuropsychological tests. A major strength of the current study is the use of a large, multi-centric dataset.

Acknowledgments

We thank the International Consortium for Brain Mapping, the LENITEM laboratory (G. Frisoni) and the ADNI study for data. This project was supported by funding from the Ministère du Développement Économique, de l'Innovation et de l'Exportation du Québec.

REFERENCES

1. Vellas, B., et al. Lancet Neurol. 2007. **6**(1): p. 56-62
2. Weiner, M., et al. 2005, Alzheimer's Association.
3. Chetelat, G. and J.C. Baron. Neuroimage, 2003. **18**(2): p. 525-41.
4. Davatzikos, C., et al.. Neurobiol Aging, 2008. **29**(4): p. 514-23.
5. Duchesne, S. 2009. Orlando, FL: SPIE Society.
6. Mueller, S.G., et al. Alzheimers Dement, 2005. **1**(1): p. 55-66.
7. Mazziotta, J.C., et al. Neuroimage, 1995. **2**(2): p. 89-101
8. Galluzzi, S., et al. Aging Clin Exp Res, 2009. **21**(4-5): p. 266-76.
9. Jack, C.R., Jr., et al. J Magn Reson Imaging, 2008. **27**(4): p. 685-91.
10. Coupe, P., et al. IEEE Trans Med Imaging, 2008. **27**(4): p. 425-41.
11. Sled, J.G., A.P. Zijdenbos, and A.C. Evans. IEEE Transactions on Medical Imaging, 1998. **17**: p. 87-97.
12. Collins, D.L., et al. Journal of Computer Assisted Tomography, 1994. **18**: p. 192--205.
13. Aubert-Broche, B., A.C. Evans, and L. Collins. Neuroimage, 2006. **32**(1): p. 138-45.
14. Maes, F., et al. IEEE Trans Med Imaging, 1997. **16**(2): p. 187-98.
15. Chung, M.K., et al. NeuroImage, 2001. **14**(3): p. 595-606.